JGR Earth Surface

RESEARCH ARTICLE
10.1029/2025JF008705

Climate-Change Projections of Flow Distribution Across the Rhine Delta

M. Kifayath Chowdhury[1], **Astrid Blom**[1], **Clàudia Ylla Arbós**[1,2], **and Ralph M. J. Schielen**[1,3]

[1]Faculty of Civil Engineering and Geosciences, Delft University of Technology, Delft, The Netherlands, [2]AXA Climate, Paris, France, [3]DG Rijkswaterstaat, Ministry of Infrastructure and Water Management, Utrecht, The Netherlands

Key Points:

- In the Rhine delta, climate change is projected to overtake human interventions as the dominant factor shaping flow partitioning
- Sea level rise outweighs projected hydrograph shifts as the dominant climate-related driver of change in flow partitioning
- Discharge in the Waal, the Rhine delta's main branch, is projected to keep increasing under future climate scenarios

Supporting Information:

Supporting Information may be found in the online version of this article.

Correspondence to:

M. K. Chowdhury,
kifayath.buet@gmail.com

Citation:

Chowdhury, M. K., Blom, A., Arbós, C. Y., & Schielen, R. M. J. (2026). Climate-change projections of flow distribution across the Rhine delta. *Journal of Geophysical Research: Earth Surface*, *131*, e2025JF008705. https://doi.org/10.1029/2025JF008705

Received 29 JUN 2025
Accepted 5 MAR 2026

Author Contributions:

Conceptualization: M. Kifayath Chowdhury, Astrid Blom, Ralph M. J. Schielen
Data curation: M. Kifayath Chowdhury
Formal analysis: M. Kifayath Chowdhury
Funding acquisition: Astrid Blom, Ralph M. J. Schielen
Investigation: M. Kifayath Chowdhury
Methodology: M. Kifayath Chowdhury, Astrid Blom, Clàudia Ylla Arbós
Project administration: Astrid Blom, Ralph M. J. Schielen
Resources: Astrid Blom, Ralph M. J. Schielen
Software: M. Kifayath Chowdhury

Abstract We project climate-driven changes in flow and sediment partitioning across the Rhine delta using a hybrid one-dimensional model informed by two-dimensional sediment-partitioning data. Simulations spanning 150 years and 540 km show a continued shift of discharge toward the Waal branch, while the effects of historical interventions gradually diminish. Climate impacts on flow division emerge around 2050 and intensify thereafter: by 2150, the IJssel is projected to convey approximately up to 17% less discharge under low-flow conditions, whereas the Waal may receive up to 6% more. Although hydrograph changes have limited influence on flow partitioning, they markedly increase channel-bed erosion by coarsening the sediment flux delivered to the bifurcation region and enhanced sensitivity to shear-stress gradients across the bifurcation. Consequently, climate forcing, particularly sea-level rise, overtakes past interventions as the dominant driver of future flow partitioning and bed level adjustment. These results have direct implications for long-term water management, navigation, and ecological resilience in the Rhine delta.

Plain Language Summary Bifurcations are where rivers split into two branches and control how water is spread across a delta. This study looks at how climate change will affect water flow across the Rhine delta in the Netherlands over the next 150 years. We find that the widest branch (the Waal) will get more water over time (up to a 6% increase), while the narrowest branch (the IJssel) will lose up to 17% of its water during low-flow conditions by 2150. This study shows how climate change is gradually becoming the main driver of the division of water across the river delta, replacing the influence of human activities. Understanding these effects is crucial for managing rivers in the future, as they will affect flood safety, freshwater supply, and shipping. This research may help engineers and policymakers plan for a changing climate to ensure safe and sustainable water management.

1. Introduction

Deltas have long been focal regions of human settlement and economic development (Best, 2019; Edmonds et al., 2020). However, they are increasingly vulnerable to climate change due to rising sea levels, altered flow regimes, and shifts in both the magnitude and grain-size distribution of sediment fluxes (Chadwick et al., 2020; Edmonds et al., 2010; Liang et al., 2016; Tessler et al., 2018; Woodruff et al., 2013). Understanding how these external stressors interact with the internal organization of deltaic systems is critical for assessing their long-term stability and resilience. Structurally, a delta comprises a distributary channel network characterized by a series of bifurcations that partition flow and sediment among its branches. Each bifurcation governs the distribution of discharge and sediment to downstream branches while simultaneously setting the base level for upstream channels (Arkesteijn et al., 2019; Wang et al., 1995), thereby exerting a primary control on delta morphology and evolution.

Previous studies have often examined this partitioning of flow and sediment using idealized single-bifurcation configurations with uniform sediment size (e.g., Bolla Pittaluga et al., 2003; Kleinhans et al., 2008; Van der Mark & Mosselman, 2013; Wang et al., 1995). These one-dimensional (i.e., aimed at changes along the flow direction) models require adoption of a so-called nodal point relation, which prescribes how sediment flux just upstream of a bifurcation is distributed among the downstream branches. Such a relation is necessary in one-dimensional models: while flow partitioning can be computed directly, sediment flux division must be specified empirically.

Idealized bifurcation models have also provided valuable insights into the number of stable equilibrium configurations and how systems evolve toward these states (Bolla Pittaluga et al., 2003; Ragno et al., 2023; Schielen

Supervision: Astrid Blom, Ralph M. J. Schielen
Validation: M. Kifayath Chowdhury
Visualization: M. Kifayath Chowdhury, Astrid Blom, Clàudia Ylla Arbós
Writing – original draft: M. Kifayath Chowdhury
Writing – review & editing: M. Kifayath Chowdhury, Astrid Blom, Clàudia Ylla Arbós, Ralph M. J. Schielen

& Blom, 2018; Wang et al., 1995). Particularly, Wang et al. (1995) was a seminal work, framing a bifurcation system as a stability problem, recognizing the significance of a nodal point relation, and demonstrating the existence of multiple equilibrium states. Subsequent studies of idealized bifurcations with mixed-size sediments have revealed more complex stability properties and additional stable configurations compared with unisize sediment conditions (Blom et al., 2024; Ragno et al., 2023; Schielen & Blom, 2018), highlighting how sediment heterogeneity can fundamentally alter bifurcation dynamics.

Field studies at deltaic and braided river bifurcations have highlighted several key processes. These include: (a) strong coherent secondary circulation cells around bifurcations, as observed in the Wax Lake delta (Chowdhury et al., 2022); (b) methods for constraining flow partitioning from in situ and remotely sensed data, demonstrated at the Selenga River delta (Dong et al., 2020); (c) water discharge as the most reliable field-based indicator for partitioning total, suspended, and bedload sediment transport (Dong et al., 2020); (d) variation of flow partitioning ratio with upstream water discharge (Hackney et al., 2017) and its correlation with differences in bifurcate width (Zolezzi et al., 2006); (e) the role of the dominant sediment transport regime in bifurcation development, as shown in the Mekong and Rio Paraná rivers (Hackney et al., 2017; Szupiany et al., 2012); and (f) the influence of bend sorting upstream of the bifurcation on sediment partitioning, observed in the Rhine River, with coarser sediment fractions showing a preference for being transported into the bifurcate that takes off from the outer bend (Frings & Kleinhans, 2008). Observations in a two-bifurcation system (upper Rhine delta) further indicate that peak flows can trigger abrupt changes in channel erosion rates and flow partitioning, followed by a gradual adjustment of the system toward new equilibrium conditions (Blom et al., 2024; Chowdhury et al., 2023).

Because deltaic channels have mild bed slopes, backwater effects play a prominent role in modifying the water-surface gradient and regulating main-channel deposition and erosion, ultimately influencing bifurcation dynamics (Edmonds, 2012; Hoyal & Sheets, 2009; Kleinhans et al., 2013). Differences in cross-sectional area between bifurcates (including channel width and bed level) also control flow partitioning, both in delta networks (Barile, Passalacqua, et al., 2025; Dong et al., 2020) and in single bifurcations (Schielen & Blom, 2018; Wang et al., 1995). Typically, the wider and deeper bifurcate receives a larger proportion of the flow due to its greater conveyance. When bifurcates have the same base level, the shorter branch tends to attract more flow because of its steeper slope (Durante et al., 2025; Edmonds, 2012). Sediment partitioning is controlled by a combination of factors: the flow partitioning (Bolla Pittaluga et al., 2003; Schielen & Blom, 2018; Wang et al., 1995), branch widths (Barile, Passalacqua, et al., 2025; Miori et al., 2006; Schielen & Blom, 2018; Wang et al., 1995), transverse bed slope immediately upstream of the bifurcation (Bolla Pittaluga et al., 2003), the presence of bends and associated bend sorting (Frings & Kleinhans, 2008; Kleinhans et al., 2008), and the offtake angles of the bifurcates (Van der Mark & Mosselman, 2013).

In deltaic networks with multiple bifurcations, interactions between bifurcations strongly influence their development (Ragno et al., 2022; Salter et al., 2018). The strength of this feedback depends on the distance between bifurcations: when bifurcations are close together, changes at a downstream bifurcation rapidly affect flow partitioning upstream, resulting in relatively strong feedback. For widely spaced bifurcations, the water surface slope in between is less affected, and flow partitioning responds more slowly. Interactions between bifurcations can sometimes lead to chaotic network dynamics, where small perturbations amplify and the system becomes difficult to predict (Salter et al., 2020). In contrast, the distance from the upstream bifurcation to the sea has a stronger influence on its stability than inter-bifurcation feedback (Durante et al., 2025).

The long-term geomorphic evolution of deltaic networks is strongly influenced by climate-driven changes in hydrographs and rising sea levels (Edmonds et al., 2010, 2022; Salter et al., 2018; Van de Lageweg & Slangen, 2017). In particular, most climate projections indicate an increase in the magnitude and frequency of peak flows (Buitink et al., 2023; IPCC, 2023), which can substantially alter flow partitioning within bifurcating systems (Blom et al., 2024; Chowdhury et al., 2023). These observations indicate that climate-induced changes in peak discharge are likely to play a key role in shaping the future development and stability of delta networks, emphasizing the importance of understanding bifurcation dynamics under extreme flow conditions.

To evaluate geomorphic response to climate change in regulated rivers, Ylla Arbós et al. (2023) developed an assessment framework and applied it to the Lower Rhine. While bifurcation dynamics were represented in a simple form, their results suggest that historical engineering works will continue to dominate channel adjustment through 2100, mainly through ongoing incision. They also showed that channel adjustment to engineering

measures slows as the system approaches equilibrium, while climate-driven response accelerates, with hydrograph changes exerting a stronger influence than sea-level rise.

A key insight from this assessment framework is the need to use measured data to constrain channel responses to historical engineering interventions, enabling clearer separation of climate-driven trends from human-induced adjustments. This is particularly important in engineered systems such as the Rhine, where fixed planform and channel confinement cause past interventions to dominate present-day morphodynamic behavior (Chowdhury et al., 2023; Ylla Arbós et al., 2021). However, in deltaic rivers with multiple bifurcations, the relative influence of engineering measures versus climate forcing on future flow and sediment partitioning remains poorly understood. Clarifying this interplay is essential for predicting the long-term resilience of bifurcating river systems.

Our objective is to quantify how climate-driven changes in river discharge regimes and sea-level affect flow partitioning in a fixed-planform, fixed-width deltaic river system over the next 150 years. We extend the work of Ylla Arbós et al. (2023) by expanding the modeled Rhine domain from 300 to 540 km and explicitly including the two key bifurcations, Pannerdense Kop and IJsselkop. We use a one-dimensional model tailored to large spatial scales and century-scale dynamics. Incorporating both bifurcations enables feedback between branches to emerge, while sediment-partitioning relationships derived from two-dimensional model data improve the representation of bifurcation behavior. Section 2 introduces the study area, Section 3 outlines the climate scenarios, Section 4 describes model development, and Section 5 presents the projected system response.

2. The Lower Rhine System

The River Rhine flows from the Swiss Alps to the North Sea, with the Niederrhein reach entering the Netherlands from Germany near Lobith (river km 858) as the Bovenrijn, which marks the start of the Rhine delta (Figure 1). Our domain (Figure 1b) extends from Bonn (Germany, river km 640) to its downstream boundaries in the Waal branch (at Vuren, Netherlands), the Nederrijn-Lek branch (at Schoonhoven, Netherlands), and the IJssel branch (Keteldiep, Netherlands).

At the Pannerdense Kop bifurcation (river km 867.5), the Bovenrijn splits into the Waal and Pannerden Canal. The latter branch then bifurcates at the IJsselkop bifurcation into the Nederrijn-Lek and IJssel branches, located 11 km downstream. We refer to the Niederrhein, Bovenrijn, Waal, Pannerden Canal, Nederrijn-Lek, and IJssel as the Lower Rhine system. Two branches flow into the North Sea, while the IJssel branch flows into the IJssel Lake. The Pannerdense Kop bifurcation is about 160 km (measured along the Waal) upstream of the North Sea, whereas the IJsselkop is approximately 150 km (measured along Nederrijn-Lek) upstream of the North Sea and 118 km upstream of the IJssel Lake. The Waal is the widest branch, with an average main-channel width of approximately 270 m, whereas the IJssel is the narrowest, with an average width of 105 m (Chowdhury et al., 2023). Mean main-channel width of the Pannerden Canal and Nederrijn bifurcates are 130 and 154 m, respectively.

Downstream of Bonn, Germany (Figure 1), the channel bed features Tertiary fine sands and Quaternary gravel and coarse sands (Frings et al., 2014). The Niederrhein bed surface predominantly consists of coarse gravel, transitioning downstream to fine and coarse sands in the gravel-sand transition region (Frings, 2011; Ylla Arbós et al., 2021). Both the Niederrhein and the bifurcation region exhibit a mobile armor (Frings et al., 2014; Gruijters et al., 2001, 2003; Parker & Sutherland, 1990). The Pannerden Canal and IJssel branches take off from an outer bend of the upstream channel, where lateral bend sorting (Parker & Andrews, 1985) preferentially transports coarse sediment into these bifurcates (Kleinhans et al., 2008), resulting in relatively coarse upstream regions (Chowdhury et al., 2023; Frings & Kleinhans, 2008).

Flow in the Rhine River is driven by glacial melt, snow-melt, and rainfall (Stahl et al., 2022). At Lobith, the mean annual discharge is 2,210 m^3/s, with a mean annual peak of 6,540 m^3/s (Chowdhury et al., 2023). The highest recorded discharge is 12,600 m^3/s, measured in 1926.

The Lower Rhine has a long history of interventions, including construction of levees, groynes, weirs, fixed beds, channel shortening, dredging, and nourishments (Chowdhury et al., 2023; Ten Brinke, 2005; Ylla Arbós et al., 2021). This has resulted in a fixed channel planform and width, and a channel response governed by ongoing channel bed incision and bed surface coarsening (Chowdhury et al., 2023; Frings et al., 2014; Quick et al., 2020; Ylla Arbós et al., 2021).

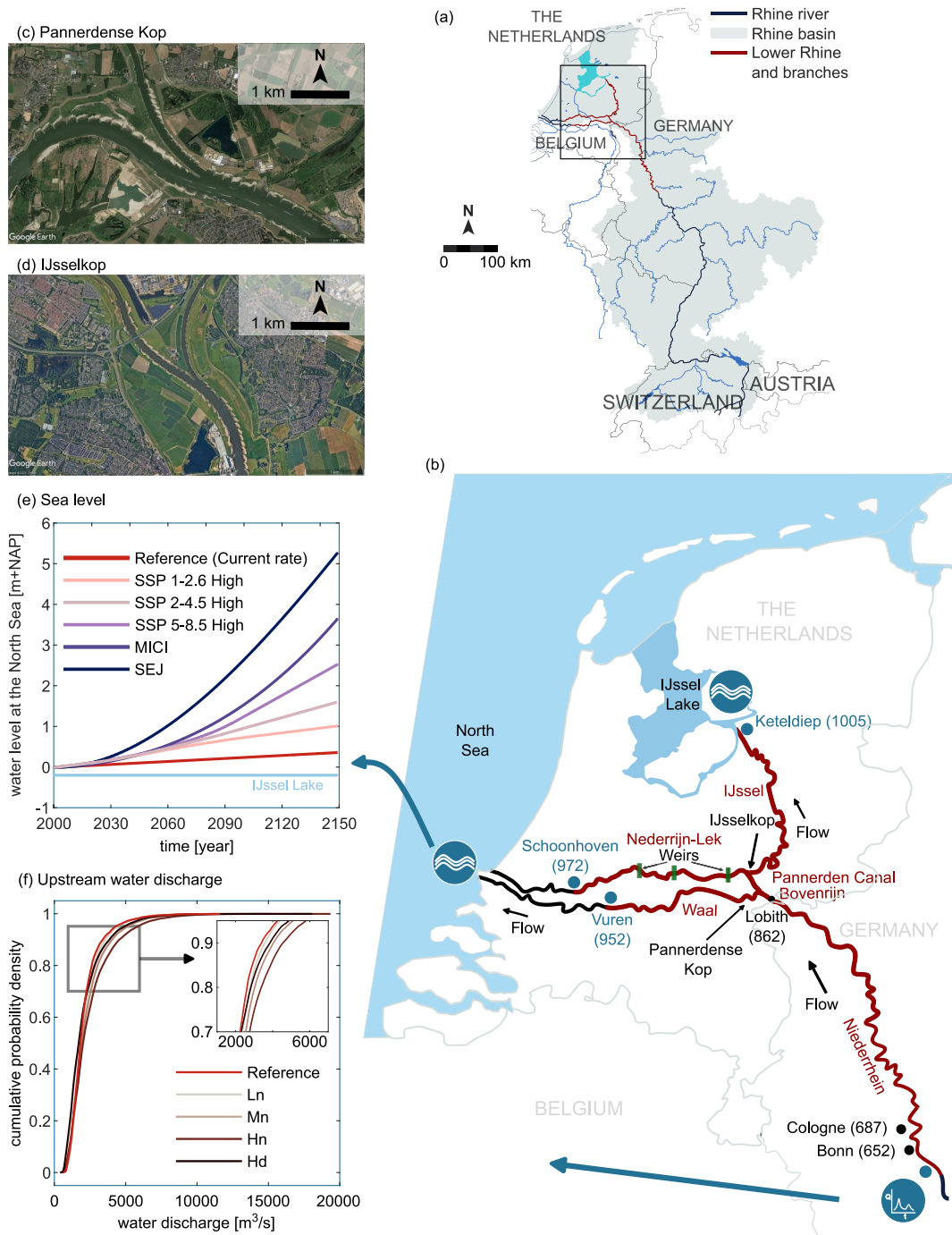

Figure 1. Lower Rhine River with climate scenarios: (a) the Rhine River basin; (b) Lower Rhine River, with numbers in parentheses indicating the distance or *river km* from Lake Constance (Bodensee); (c, d) aerial images of the Pannerdense Kop and IJsselkop bifurcations, respectively; (e) sea-level rise scenarios (Van Dorland et al., 2023); and (f) hydrograph scenarios for 2100 at Lobith (Buitink et al., 2023). Panels (c, d) are from Google Earth, accessed on 29 Oct 2024.

Three weirs in the Nederrijn-Lek branch (Figure 1b), constructed between 1950 and 1970, help maintain suitable shipping conditions and freshwater supply for the IJssel during low flows and a minimum flow in the Nederrijn-Lek branch to mitigate salt intrusion (Ten Brinke, 2005). Operation (i.e., closure and lifting) of the weirs is a function of the water level at Lobith. Following Chowdhury et al. (2023), we consider the following two operation modes for the upstream weir (at Driel, situated 12.5 km downstream of the IJsselkop bifurcation): (a) a fully

closed Driel weir (Lobith water level smaller than 8.6 m NAP, where NAP denotes Normal Amsterdam Level and is the typical Dutch reference level), and (b) a fully open weir (for Lobith water level larger than 10 m NAP). This open or closed weir regime results in a bimodal behavior regarding flow partitioning (see Section S1 in Supporting Information S1). This is because the closed weir condition diverts a larger share of the Lobith discharge into the IJssel, at the expense of the Nederrijn-Lek branch. A closed Driel weir also increases the Waal discharge, as the associated backwater extends upstream beyond the Pannerdense Kop bifurcation (Chowdhury et al., 2023).

Since the mid-1990s, the Pannerden Canal has eroded more slowly than the Waal branch, with flow increasingly favoring the Waal (Blom et al., 2024; Chowdhury et al., 2023). This shift seems to be related to the peak flows in 1993, 1995, and possibly 1998.

3. Scenarios for Hydrograph Change and Sea-Level Rise

The IPCC global climate scenarios project future changes based on emissions and socio-economic factors (Masson-Delmotte et al., 2023). High emissions lead to substantial warming, intensified droughts, floods, and rapid sea-level rise, while low emissions show milder impacts.

The KNMI'23 scenarios for the Netherlands (Van Dorland et al., 2023) downscale the results of Global Climate Models using a regional model to capture local climate and topography. Three scenarios, SSP 1-2.6 (L), SSP 2-4.5 (M), and SSP 5-8.5 (H), represent low, moderate, and high impacts, with wet (n) and dry (d) versions for wetter and drier futures (Buitink et al., 2023; O'Neill et al., 2017; Van Dorland et al., 2023). All scenarios indicate rising climate variability, with high-impact scenarios showing pronounced seasonal extremes (i.e., wetter winters and drier summers). Sea-level rise along the Dutch coast is projected to reach 0.26–2.5 m by 2100 relative to the Van Dorland et al. (2023) reference period 1995–2014.

These regional climate scenarios are translated into Rhine hydrographs at Lobith using a hydrological model (Buitink et al., 2023; Van Verseveld et al., 2024), with 1990–2020 as their reference climate. Each scenario is represented by 8 ensembles of 30-year discharge time series for future time horizons 2050, 2100, and 2150. In our analysis, we use the Ln, Mn, Hn, and Hd hydrograph scenarios (Figure 1f). We linearly extrapolate the flow duration curve of the low-impact (L) scenario to 2150, as it is originally available up to 2100 due to the negligible climate signal beyond that horizon (Buitink et al., 2023).

We assess sea-level rise impacts using the 95% uncertainty upper limit of the SSP 1-2.6, SSP 2-4.5, and SSP 5-8.5 scenarios (Figure 1e). We also consider two Low Probability High Impact scenarios, SEJ and MICI, which include accelerating factors beyond standard models (Van Dorland et al., 2023).

Section S2 in Supporting Information S1 provides more detailed information on the adopted hydrograph and sea-level rise scenarios.

4. The Model

This section outlines the model setup, with Section S3 in Supporting Information S1 offering further details on the model choices.

We employ a one-dimensional approach to meet the demands of 150-year simulations over a 540-km domain with multiple branches and numerous control scenarios. A one-dimensional model focuses solely on changes along the main flow direction, making it particularly suitable for studying broad, long-term patterns.

We extend the model by Ylla Arbós et al. (2023) and include the Pannerdense Kop and IJsselkop bifurcations, increasing the domain from 300 to 540 km. Our model is informed on sediment partitioning at the bifurcations using data from a two-dimensional model of the bifurcation region (Becker, 2021; Ottevanger et al., 2015). We smooth channel width, floodplain width, initial bed level, and initial surface and substrate size fraction contents (Figure 2a and Figures S3 and S4 in Supporting Information S1), as we are interested in large-scale changes rather than localized variations. We preserve discontinuities in these properties at the bifurcations where spatial changes in bed level (e.g., bed step) and surface grain size are typical (Barile, Passalacqua, et al., 2025; Chowdhury et al., 2023; Frings & Kleinhans, 2008; Zolezzi et al., 2006). We also preserve abrupt spatial changes in width and discontinuities at the weirs (Figure S3 in Supporting Information S1). We neglect the Rhine River's tributaries within the domain as their contribution to the water discharge and bed material load is limited (Section S3 in Supporting Information S1).

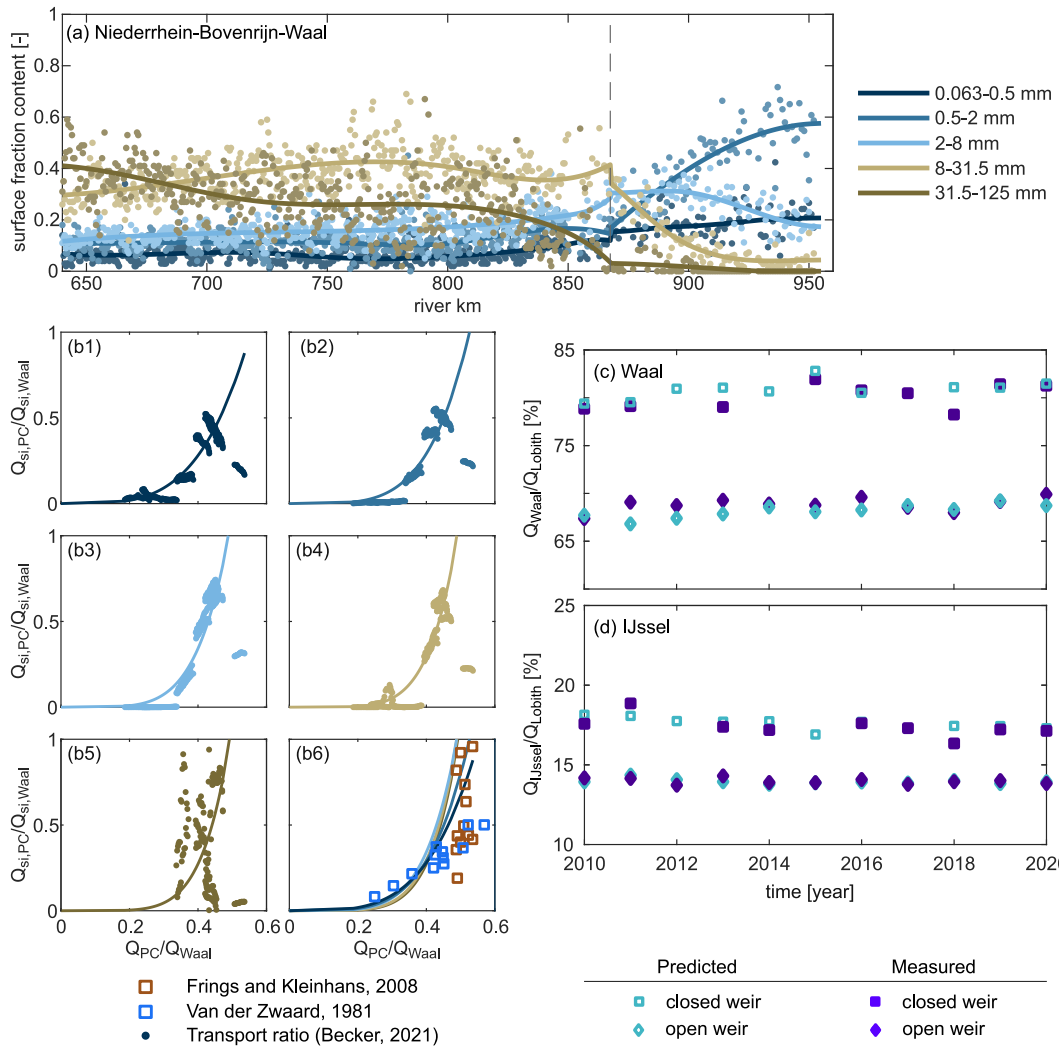

Figure 2. Initial conditions, internal boundary conditions, and model calibration: (a) initial volume fraction content of the five grain size classes in the bed surface sediment; (b1–5) internal boundary conditions for each of the five grain size classes (with grain size reflected by color and legend of subplot a), represented by nodal point relations linking the grainsize-specific Pannerden Canal-to-Waal sediment supply ratio (Q_{siPC}/Q_{siWaal}) to the Pannerden Canal-to-Waal discharge ratio (Q_{PC}/Q_{Waal}). The discharge ratio at the Pannerdense Kop increases with Lobith discharge (Chowdhury et al., 2023), implying that the Pannerden Canal receives a larger share of the Lobith discharge with increasing Lobith discharge (Figure S12e in Supporting Information S1). Data points refer to sediment transport data (averaged over a 1-km distance right downstream of the bifurcation) from the two-dimensional numerical model by Becker (2021); (b6) comparing grainsize-specific nodal point relations with field data (Frings & Kleinhans, 2008) and scaled laboratory experiments (Van der Zwaard, 1981), related to total sediment transport rates; (c, d) model calibration based on the flow partitioning at the two bifurcations.

Key simplifications include the following: channel and floodplain widths remain constant over time; we neglect factors such as subsidence, uplift, delta formation, salt intrusion, tides, and particle abrasion; only bed-material load is considered; the sediment mixture consists of five grain size classes (with characteristic grain sizes equal to 0.5, 1.2, 4.9, 15.5, and 38.7 mm); for each bifurcation, the partitioning of a grain size class follows a power-law nodal point relation; and erosion and deposition are restricted to the main channel (i.e., floodplain bed level remains constant).

Flow is computed using the steady solution to the one-dimensional shallow water equations (Saint Venant, 1871). Changes in bed level and bed surface grain size follow from the equation for grainsize-specific sediment conservation (Hirano, 1971). A set of bookkeeping layers keeps track of temporal changes in the bed sediment grain size distribution (Viparelli, Haydel, et al., 2010; Viparelli, Sequeiros, et al., 2010). We apply the numerical

software SOBEK-RE (Mulatu et al., 2020; Sloff, 2006; Ylla Arbós et al., 2023) as it allows for floodplain flow, mixed-size sediment, and a steady solution to the flow equations. The latter conveniently reduces simulation time for the 150-year simulations. Grainsize-specific sediment transport is calculated using a relation that includes a threshold of motion and hiding (see Section S3 in Supporting Information S1).

The initial state of the model represents the year 2000. Bed level is based on field data averaged over 1998–2002 for the Dutch Rhine, and 2000–2002 for the German Rhine. The initial surface grain size distribution (Figure 2a and Figures S4a and S4b in Supporting Information S1) is derived from Niederrhein data acquired over the period 1990–2010 (Frings et al., 2014) and from 2020 for the Dutch reaches (Ylla Arbós et al., 2021). Substrate sediment composition for the Niederrhein-Bovenrijn branches stems from 1990 to 2010 data (Frings et al., 2014), and it matches the surface sediment for the downstream reaches.

We introduce a 150-year reference case spanning from 2000 to 2150. Boundary conditions of the reference case include a cycled hydrograph with a 20-year period (1994–2013) with statistical properties similar to the Buitink et al. (2023) reference period (see Section S3 in Supporting Information S1). This allows for capturing flow rate variability and adding a climate signal to the hydrograph in the climate scenario runs. We use Lobith discharge data at the model upstream boundary, as our focus is on the bifurcation region. The grainsize-specific sediment flux at the upstream boundary equals the equilibrium load or normal-flow load distribution (Blom et al., 2017) for the initial channel geometry.

Sediment partitioning at bifurcations is controlled by complex two-dimensional (or even three-dimensional) processes (Van der Mark & Mosselman, 2013). The adoption of a one-dimensional model requires an internal boundary condition that prescribes how the sediment flux of each grain size class divides at a bifurcation (Ragno et al., 2023; Schielen & Blom, 2018; Wang et al., 1995). For simplicity, we assume that each grain size class follows a grainsize-specific power-law nodal point relation (Figure 2b), informed by data from a two-dimensional model of the bifurcation region (Becker, 2021; Ottevanger et al., 2015). The grainsize-specific nodal point relations take the following form:

$$\left[\frac{Q_{si1}}{Q_{si2}} = \alpha_i \left(\frac{Q_1}{Q_2}\right)^{k_i}\right]_{\text{bifurcation}} \tag{1}$$

where subscripts 1 and 2 indicate the two downstream branches (or bifurcates) of each of the two bifurcations, Q_{si1} and Q_{si2} are the grainsize-specific sediment supply to bifurcates 1 and 2, i refers to one of the five grain size classes, Q_1 and Q_2 are the water discharges to bifurcates 1 and 2, and α_i and k_i are grainsize-specific constants calculated through comparison with the two-dimensional model data (Table S1 in Supporting Information S1). Mass is conserved at each bifurcation.

The coarsest grain size class (31.5–125 mm) data does not allow for a strong fit (Figure 2b5), yet less than 3% of the sediment flux reaching the bifurcation region consists of this size class (Frings et al., 2014), implying that the weak fit has limited impact on overall results. The preference for the coarse size classes to be transported into the Pannerden Canal (and into the IJssel branch vs. the Nederrijn-Lek branch) is stronger than for the finer sizes (Figure 2b6 and Figure S6f in Supporting Information S1). The resulting nodal point relations also compare reasonably well (Figure 2b6) with field data on total transport rates (Frings & Kleinhans, 2008) and scaled laboratory experiments (Van der Zwaard, 1981).

For simplicity, the estuarine zone is not included in the model domain, and therefore, the downstream model boundaries do not coincide with locations for which sea-level rise projections are directly available. The two western downstream model boundaries are located 60 and 75 km upstream of the North Sea. Sea and lake level scenarios are translated into model base levels following the approach of Ylla Arbós et al. (2023), which is explained in Section S3 of Supporting Information S1. In particular, we estimate downstream water levels using a backwater-based approximation that links model boundary water levels to North Sea water levels derived from storm-surge data (Equation S6 in Supporting Information S1). We subsequently apply this relationship to translate projected sea-level rise at the North Sea into corresponding model boundary water levels. This approach assumes that the backwater relation remains unaffected by future bed-level change within the estuarine zone, which is an assumption that simplifies the analysis but should be examined in future work. The reference case uses

the current rate of sea-level rise at the North Sea equal to 2.5 mm/year (Van Dorland et al., 2023), while the water level in the IJssel Lake remains constant and unaffected by sea-level rise (Figure 1e).

We account for fixed layers by imposing a coarse immobile substrate, sediment nourishments along the Niederrhein-Bovenrijn branch, and dredging in the lower Waal branch. We include the three weirs in the Nederrijn-Lek branch through operating rules based on water level at Lobith (Section S3 in Supporting Information S1). When completely or partially closed, the weirs block the sediment flux completely and, when completely lifted, allow for unhindered sediment transport.

We adopt a 10-year model spin-up period (2000–2010) to allow the system to adjust, reducing transient effects from mismatches between the initial conditions and model relations, thus achieving more realistic results. We calibrate the pre-factor and critical Shields stress in the sediment transport relation and bed friction against measured flow partitioning at the two bifurcations and temporal change in bed level relative to 2009–2011 (order of magnitude and sign) over the period 2010–2020. We have calibrated the longitudinal profile of the total bed friction, and the resulting values remain constant over time and across different flow regimes. This simplified approach for constraining total friction can be refined in future studies. Flow partitioning trends at both bifurcations agree well with measured data (Figures 2c and 2d),

Verification involves a comparison of predicted and measured water levels at four locations in the Bovenrijn, Waal, Nederrijn-Lek, and IJssel branches over the same period (Figures S12a–S12d in Supporting Information S1). Although the one-dimensional model is designed to capture variations primarily along the main flow direction, it incorporates a simplified representation of overbank conveyance and floodplain storage. Comparisons with observations show systematic overestimation of water levels during medium- and high-discharge conditions, together with an overprediction of discharge into the Pannerden Canal (Figure S12 in Supporting Information S1). These discrepancies may arise in part from the use of a steady-flow approximation, which assumes instantaneous transmission of upstream discharge variations and neglects the diffusive and attenuating characteristics of real flood-wave propagation. They may also reflect the fundamental limitations of one-dimensional formulations in reproducing overbank conditions. Section S3 in Supporting Information S1 provides further information on numerical parameter settings, spin-up, calibration, and verification.

Our climate scenario runs (Figures 1e and 1f) involve four hydrograph scenarios, Ln, Mn, Hn, Hd (Buitink et al., 2023), four sea-level rise scenarios, SSP 1-2.6, SSP 5-8.5, MICI, and SEJ (Van Dorland et al., 2023), and four combined scenarios (SSP 1-2.6-Ln, SSP 2-4.5-Mn, SSP 5-8.5-Hn, and SEJ-Hn). We add the climate signals of the hydrograph scenarios to the cycled hydrograph of the reference case following the procedure of Ylla Arbós et al. (2023), which is detailed in Section S3 of Supporting Information S1. We do not consider (climate) scenarios for the sediment flux, as associated effects are unlikely to reach the bifurcation region within our 150-year projections (Ylla Arbós et al., 2023).

5. Projected Response of the Two-Bifurcation System

In addressing climate-change impact on flow partitioning over the bifurcates, we denote the two Driel weir regimes (closed and lifted weir conditions) as the "low-flow" and "high-flow" regimes, respectively. The short time scale fluctuations in our projections of the flow partitioning (Figure 3) relate to changes in water discharge throughout the year, and we apply a Loess fit (Cleveland & Devlin, 1988) to the flow partitioning projections over a 50-year span to identify temporal trends in our projections.

In the reference case, the Waal-to-Lobith discharge ratio increases with time, by approximately 3% by 2150 (Figure 3, left column, red lines). Simultaneously, the IJssel-to-Lobith discharge ratio decreases by 2.4% by 2150 in the low-flow regime, while relative IJssel discharge is barely affected and slightly increases under the high-flow regime. The rates of change slowly decrease with time, which holds for both branches and both weir regimes. The slowing of change seems to be associated with the system approaching equilibrium. In addition, the Pannerdense Kop bifurcation region is projected to erode (Figures 4a and 4g–4i), the sediment flux arriving at the bifurcation region strongly declines with time (Figure 4c), the bed surface continues to coarsen with time (Figure 4e), while the transported sediment in the bifurcation region slightly fines with time.

Overall, we see that, in the reference case, current trends continue. The Waal branch is projected to continue attracting an increasing proportion of the Lobith flow (Figure 3, left column, red lines), which is associated with the Waal branch eroding faster than the Pannerden Canal (Figures 4h and 4i). The temporal coarsening of the bed

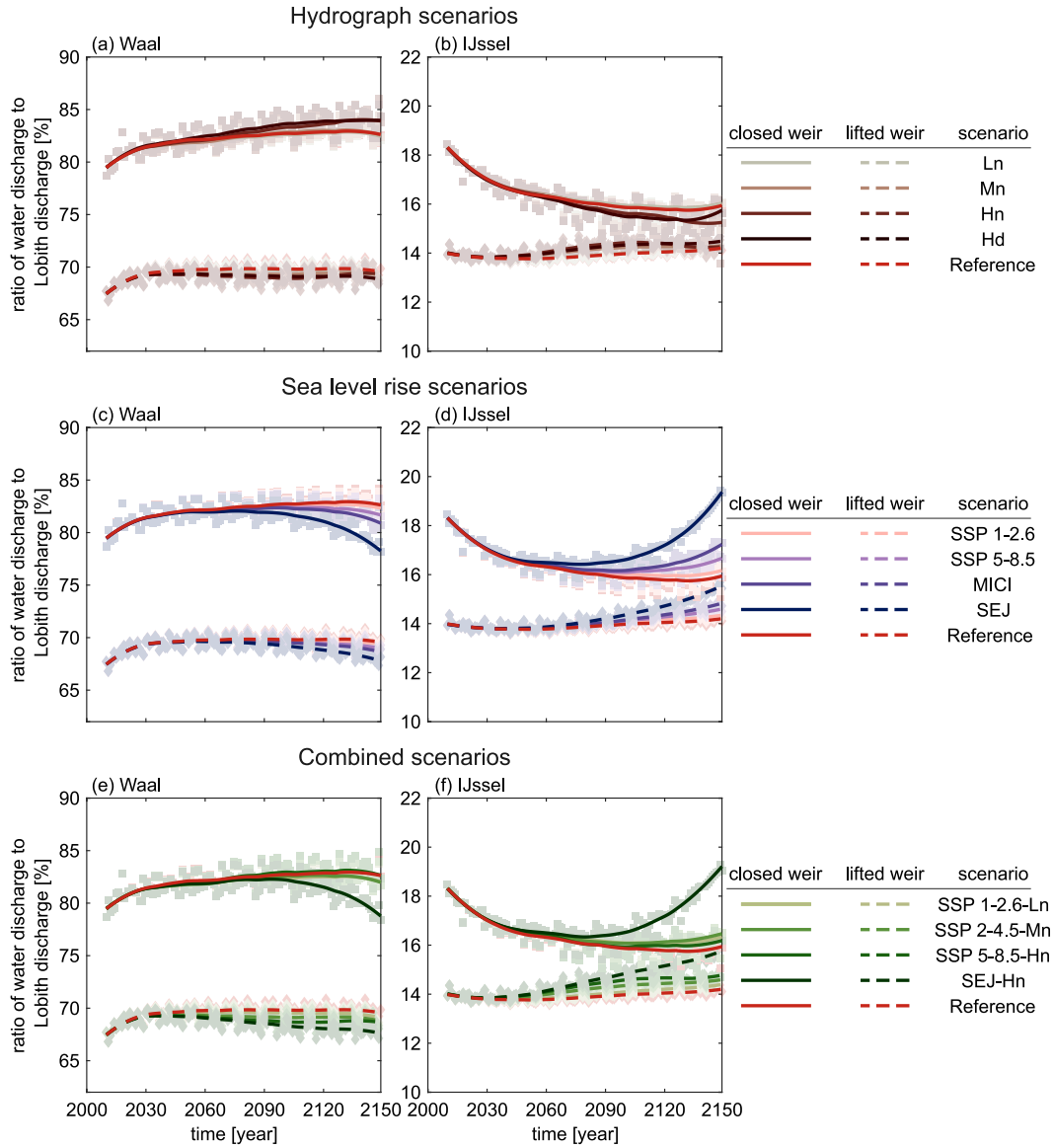

Figure 3. Projections of Waal-to-Lobith discharge ratio (left column) and IJssel-to-Lobith discharge ratio (right column) as a function of time for (a, b) hydrograph scenarios; (c, d) sea-level rise scenarios; and (e, f) combined scenarios. Light-colored squares and diamonds are low-flow and high-flow regimes, or closed-weir and open-weir projections, respectively, with continuous and dotted lines showing Loess regressions to projected data (with a 50-year span). The projections for mild climate change scenario often overlap with the reference case.

surface sediment (Chowdhury et al., 2023; Ylla Arbós et al., 2021) is projected to persist (Figure 4e). The decline of the annual bed material flux in the reference case (Figure 4c) is remarkable and may be due to one or more of the following causes: (a) the lagging gradual adjustment of the bed material load toward a previous decrease of the sediment supply; (b) the lagging gradual adjustment of the bed material load to a previous reduction of flow rates; (c) sediment nourishments having contributed to bed surface coarsening reducing the annual bed material load; (d) the bed material load gradually returning to values of the upstream supply after a long period of increased sediment transport due to past channel narrowing. A combination of these causes may be the most likely explanation.

The hydrograph scenarios have a very limited effect on flow partitioning compared to the reference case (Figures 3a and 3b). Climate impacts do become apparent in bed level from approximately 2050 (Figures 4a and 4b) when the sediment flux arriving at the bifurcation region, which is significantly coarser than that of the

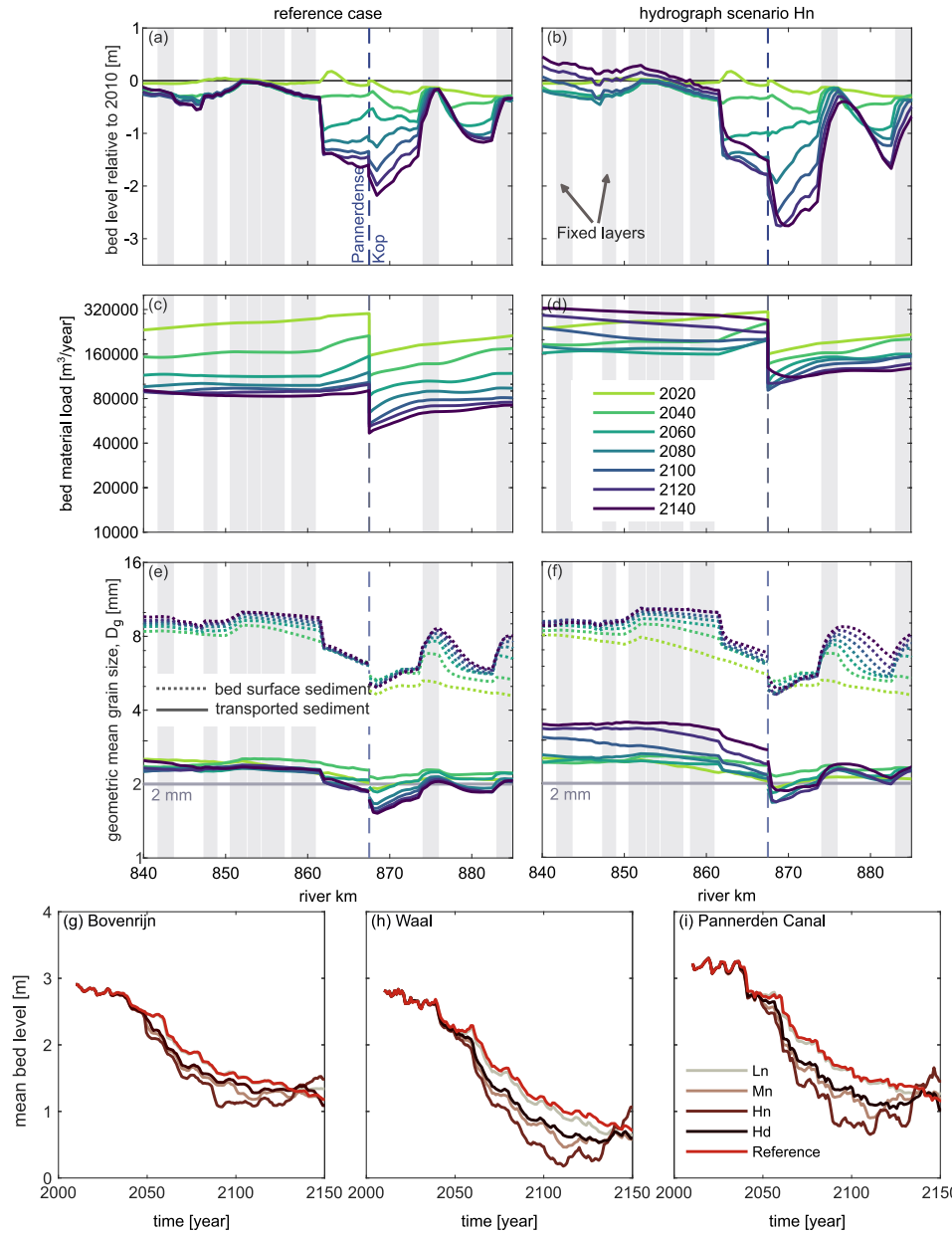

Figure 4. Projections for the reference case (left column) and the Hn hydrograph scenario (right column) over the Niederrhein-Bovenrijn-Waal branches: (a, b) bed level relative to 2010; (c, d) annual bed material load; and (e, f) geometric mean grain size of bed material load and bed surface sediment. Subfigures (g, h, i) show the temporal change of bed level for Bovenrijn, Waal, and Pannerden Canal 500 m upstream and downstream of the bifurcation, respectively. Subfigures (c–f) show 20-year averaged values.

reference case (Figure 4f), triggers intensified erosion in the Bovenrijn (Figures 4b and 4g). This, in turn, causes substantial bed erosion in the Pannerdense Kop bifurcation region, with variation across scenarios (Figures 4b and 4h–4i). At the upstream end of the Waal and Pannerden Canal, erosion continues at about 2 cm per year, with climate change contributing up to an additional 1 cm annually. Similar erosion rate increases between the Waal and Pannerden Canal under the hydrograph scenarios likely explain their minimal influence on flow partitioning.

In the Hn hydrograph scenario, the sediment flux arriving from upstream largely exceeds that of the reference case and is significantly coarser (Figures 4c–4f). Both these effects result from the climate-related increase of water discharges in the Hn hydrograph scenario.

The temporal coarsening of the sediment flux in the Hn hydrograph scenario (Figure 4f) enhances main-channel erosion by increasing the mismatch between the sediment supplied to the bifurcation and the local sediment-transport capacity. The fact that the Hn scenario's larger peak flows enhance main-channel erosion, and their limiting effect on bed-surface coarsening, can be understood from the following. The peak flows increase the mobility of all size fractions but also the coarsest grain-size fractions, thereby coarsening the transported sediment flux. This reduces the need for additional bed-surface coarsening to achieve sufficient mobility of coarse material (Blom et al., 2016, 2017). Because these coarse fractions travel closer to their threshold of motion, they are more sensitive to the decline in flow velocity and shear stress in the downstream direction when passing the Pannerdense Kop bifurcation. This mechanism explains the amplified erosion observed in the Waal and Pannerden Canal branches when peak flows are included.

For the sea-level rise scenarios (Figures 3c and 3d), the Waal-to-Lobith discharge ratio under the low-flow regime decreases relative to the reference case (up to 5% by 2150), while the IJssel-to-Lobith discharge ratio increases (up to 3.5% by 2150). In other words, under the low-flow regime, the Waal discharge is projected to increase less strongly compared to the reference case, and the IJssel discharge is expected to reduce less strongly. This is due to the fact that the IJssel Lake level is maintained constant, while sea-level rise impacts the other branches through backwater effects and associated upstream migrating deposition waves (Blum & Törnqvist, 2000; Schumm, 1993). As water level at the downstream boundary of the IJssel remains unchanged with rising sea level, these adjustment waves push more flow toward the IJssel upon reaching the bifurcation.

Under the high-flow regime, the sea-level rise scenarios have a similar tendency: the temporal increase of the Waal discharge is compensated with variable extent through backwater effects with upstream-migrating waves of bed level adjustment in the western branches. Similarly, the slight increase of the IJssel discharge of the reference case is enhanced by sea-level rise. Accounting for bed level change appears to be essential to assessing the effects of sea-level rise on temporal changes to the flow partitioning (Figure S15 in Supporting Information S1).

In the combined scenarios (Figures 3e and 3f), under low-flow conditions, the Waal discharge is projected to increase with time, and the difference with the reference case is negligible. Similarly, the IJssel discharge is projected to decrease under low-flow conditions, with negligible differences with the reference case. This implies that the ongoing response to past interventions continues to dominate the flow partitioning over the next 150 years under low-flow conditions. The only exception is the extreme SEJ sea-level rise scenario: in combined scenarios including this scenario, by 2150, sea-level rise compensates the Waal flow increase and IJssel flow decrease due to past interventions.

In contrast, under high-flow conditions, both sea-level rise and hydrograph changes strengthen one another, and reduce the intervention-induced flow increase in the Waal. In this, the effect of sea-level rise surpasses that of hydrograph changes.

The relative importance of peak flows was assessed by removing the upper 0.5%, 2%, and 5% of discharge values from the reference hydrograph (Figure S16 in Supporting Information S1). Peak discharges strongly drive and intensify channel-bed erosion and limit bed-surface coarsening. They, however, only modestly enhance the projected temporal changes in flow partitioning at the bifurcations. Thus, while morphodynamic responses are sensitive to the largest peak flows, long-term trends in flow partitioning exhibit only limited dependence on these extreme events. The latter seems to be due to the fact that the flow distribution across bifurcates is mostly controlled by the width-ratio of the two bifurcates (Barile, Passalacqua, et al., 2025), and to a smaller extent by differences in bed level change between the bifurcates. The fact that the flow partitioning depends on the upstream discharge (Figure S12e in Supporting Information S1) illustrates how the bifurcates' conveyance width depends on the upstream discharge.

Besides peak flows, we have also tested the sensitivity of our model results to different weir operation programs, constants in the grainsize-specific nodal point relations, the substrate sediment, and the presence and initial depth of the fixed layers (Figures S17–S22 in Supporting Information S1). We do not find a strong influence of these factors.

The influence of past interventions on the flow partitioning (represented by the reference case) remains dominant over the first few decades. As climate-change impacts accelerate and response to past interventions slows, the relative importance of climate impacts on system response grows with time and starts to exceed that of past interventions from approximately 2050 (Figures 3e and 3f).

In this assessment, changes in the Waal-to-Lobith and IJssel-to-Lobith discharge ratios may appear to be limited. However, translating these values into the relative change of the Waal and IJssel discharges indicates an up to 6% increase of the Waal discharge and an up to 17% decrease of the IJssel discharge by 2150 under low-flow conditions. Under high-flow conditions, Waal and IJssel discharges are projected to increase by up to 3.5% and 12.5%, respectively.

6. Discussion

Our analysis differs from that of Ylla Arbós et al. (2023) by expanding the model domain to include two bifurcations and additional distributary branches. Whereas their study represented the Pannerdense Kop in a highly simplified way (using linear nodal relations and imposing a downstream boundary only 1 km downstream of the bifurcation), we incorporate bifurcation feedbacks and sediment-partitioning relations derived from two-dimensional model data. This enables a more realistic representation of how changes in one branch propagate through the network.

Ylla Arbós et al. (2023) found that climate-driven changes to the hydrograph primarily affect channel-bed evolution, whereas sea-level rise has little influence. In contrast, our results indicate that sea-level rise strongly affects future flow partitioning, while hydrograph changes have only a minor effect. These outcomes are not contradictory: even if sea-level rise has limited impact on bed levels, small backwater-driven changes in water levels at the Waal and Pannerdense Kop can still substantially modify discharge division. Our findings also support Ylla Arbós et al. (2023)'s conclusion that climate-driven hydrograph changes enhance channel-bed erosion.

The current study indicates that future geomorphic development of the Rhine delta is largely driven by medium flows rather than peak flows. This appears to contrast with observations by Chowdhury et al. (2023), which suggest that a series of peak flows in the 1990s altered the erosion rate difference between the Waal and Pannerden Canal branches, leading to a subsequent gradual increase in discharge to the Waal. Our analysis focuses on future climate-driven impacts and has not attempted to reproduce 1990s conditions. Further research could investigate the role of historical peak flows in shaping trends in channel bed erosion and flow partitioning.

The role of the IJssel branch is particularly interesting, as in our analysis, its downstream end is not affected by sea-level rise, in contrast to the other bifurcates. This implies that sea-level rise results in the IJssel branch receiving a larger share of the Lobith flow. Our analysis does not include scenarios where the imposed IJssel Lake level follows sea-level rise, and we recommend further research into this aspect.

This study indicates that flow and sediment partitioning respond to climate-driven hydrograph changes and sea-level rise on similar decadal timescales—much shorter than the century-scale response proposed by De Vriend (2015). Bed-level and surface grain-size adjustments along the distributary branches are expected to occur more slowly (Barile, Redolfi, & Tubino, 2025), with rates influenced by branch length. Consistent with Van de Wiel et al. (2011), our results highlight that assessments of climate impacts on river systems require modeling domains that span multiple decades and several hundred kilometers to adequately capture these adjustment processes.

We developed a novel approach to derive grainsize–specific nodal point relations for our one-dimensional model by calibrating them directly against output from a two-dimensional morphodynamic simulation. This method allows us to incorporate, in an indirect but process-informed way, effects such as transverse bed slopes, upstream channel curvature, and bar dynamics near the bifurcation. The accuracy of these relations depends on the morphodynamic configuration remaining broadly similar to that represented in the two-dimensional model, implying that their validity may diminish over longer time horizons, which should be evaluated in future work. Nevertheless, grounding nodal point relations in two-dimensional model data provides a physically consistent basis for their application within simplified one-dimensional frameworks.

For low values of the Lobith discharge and so low values of the ratio of the Pannerden Canal discharge to Waal discharge, Figure 2b suggests that the sediment flux to the Pannerden Canal is very small or negligible relative to that of the Waal. Unfortunately, we cannot compare these model data to field observations because the latter are not available. The two-dimensional numerical model is based on a sediment transport relation with a threshold for incipient motion. Hence, it is hard to assess whether the output of the model for low shear stress values is realistic or the result of two-dimensional model choices.

For simplicity, we have not included the estuarine zone in our model domain. This implies that our downstream model boundaries are not at those locations for which we know scenarios for sea-level rise. We have applied backwater approximations to relate water level at each of the downstream model boundaries to water level at the North Sea, based on storm surge data (Equation S6 in Supporting Information S1). Subsequently, we apply this relation to approximate water levels at the downstream model boundaries based on water level at the North Sea, where the latter follows sea-level rise scenarios. In doing so, we have assumed that this relation is not affected by bed level change across the estuarine zone. This is a simplification that should be addressed in future studies.

Another point of attention is the representation of overbank flow. Although our one-dimensional model primarily describes changes along the main flow direction, it includes a simplified treatment of overbank conveyance and floodplain storage. Model–data comparisons indicate that water levels are overestimated during medium- and high-discharge conditions, accompanied by an overprediction of flow into the Pannerden Canal. These biases may also reflect the limitations inherent to representing overbank hydraulics in a one-dimensional framework. Together, these issues highlight the need for a more detailed evaluation of overbank processes in future work.

The projected reduction of the IJssel discharge during low-flow or closed-weir conditions will result in a longer time for the IJssel Lake to recharge to its desired stage. This will need attention as the IJssel Lake is the major freshwater reservoir for the Netherlands, and supports freshwater demand for roughly 30% of the country. In addition, the operation of the weirs in the Nederrijn-Lek branch will need consideration in light of projected changes to the flow partitioning and closure time of the Driel weir (Figure S23 in Supporting Information S1). During low flows, weir operation will be unable to maintain sufficient navigable depth in the IJssel branch, resulting in navigability issues for an increasing fraction of the year.

Adaptation to the projected intervention-driven and climate-driven river response is of large interest to delta regions. Mitigation measures in the Rhine delta relate to countering the ongoing increase of flow and associated channel bed erosion in the Waal branch, as well as the decreased flow in the IJssel branch. Human interventions that may help achieve this are lowering of floodplains, longitudinal training dams, and sediment nourishments (Czapiga et al., 2022a, 2022b). Such adaptation measures are beyond the scope of this study.

Overall, our one-dimensional approach with model data-based relations for sediment partitioning offers useful insights on the long-term response to climate change. Although higher-dimensional models accounting for transverse flow and sediment dynamics can more accurately capture bifurcation dynamics (Sloff & Mosselman, 2012), applying them to a 540-km domain over 150 years was not feasible at the time of our model development.

7. Conclusions

Focusing on changes along the main flow direction, we investigate the impact of climate change on an engineered river bifurcation system across a 540 km domain and a 150-year period, considering multiple climate scenarios for the flow regime and sea-level rise. To do so, we have adopted the Ylla Arbós et al. (2023) framework for assessing climate impacts on a river system. Sediment partitioning at the bifurcations in the model is informed by data from a two-dimensional numerical model that accounts for transverse flow, sediment, and bed level dynamics.

Specifically, we have assessed how climate change affects a deltaic river system with two bifurcations in the upper Rhine delta, focusing on flow partitioning between the downstream branches. We underline the need to evaluate current system changes based on measured data (e.g., channel bed erosion, changing flow partitioning) in such an analysis to be able to separate climate-driven changes from ongoing channel adjustments.

During the first decades, past interventions continue to dominate flow partitioning in the bifurcation region. From approximately 2050, climate-driven factors related to hydrograph changes and sea-level rise become more influential, with the impact of sea-level rise being dominant under high-flow conditions and impacts of hydrograph changes and sea-level rise compensating each other under low-flow conditions. The SEJ sea-level rise scenario is an exception to this, and pushes a large share of the upstream (Lobith) discharge to the IJssel branch, especially under low-flow conditions.

Projected climate-driven hydrograph changes are expected to: (a) coarsen the sediment flux arriving at the bifurcation region; (b) prevent the sediment-flux decline observed in the reference case; (c) have only a minor effect on flow partitioning; and (d) significantly increase channel bed erosion in the bifurcation region. This

behavior arises because the coarser sediment flux in these scenarios is transported closer to its threshold of motion and thus is more sensitive to the spatial decrease in shear stress across the Pannerdense Kop bifurcation. As a result, enhanced erosion develops across the bifurcation region, where the erosion magnitude varies depending on the specific hydrograph scenario.

The projected bifurcation system changes from around 2050 appear to be associated with the climate-related increased medium water discharges rather than increased maximum peak flows.

Accounting for bed level change appears to be essential when assessing the effects of sea-level rise on the flow partitioning across the Rhine delta branches.

Our results suggest that the current trend of water discharge increase in the dominant downstream branch (Waal) continues and project an up to 6% further increase in discharge to the Waal and an up to 17% decrease to the IJssel during low flows by 2150. Under low-flow conditions, the effect of past interventions largely dominates over the impact of climate change, except for the SEJ sea-level rise scenario. In the latter case, the impact of climate change compensates for the effect of past interventions by 2150. Under high-flow conditions, the effect of sea-level rise dominates over those of past interventions and climate-related hydrograph changes.

Our approach, which focuses on changes along the main flow direction, provides valuable insights into climate-driven geomorphic impacts on delta systems with bifurcations. Using data from a two-dimensional numerical model to constrain grainsize-specific nodal point relations, our method offers a pragmatic and effective framework for a foundational assessment of climate-related changes in bifurcating river systems, guiding future, more detailed research. These insights can be further enhanced by incorporating models that account for transverse flow and sediment dynamics, allowing for a more comprehensive understanding of river bifurcation processes.

Adopting a hybrid approach, combining a physically based model with a data-informed component, appears to be a promising strategy for examining and forecasting the long-term behavior of engineered, large-scale fluvial systems such as the Lower Rhine River. Although such models are still relatively new in geomorphology, they are likely to become an important and productive direction for future research.

Conflict of Interest

The authors declare no conflicts of interest relevant to this study.

Availability Statement

For measured data, we refer to the Data Availability Statements in Chowdhury et al. (2023) and Ylla Arbós et al. (2023). Model input and output files are provided in https://doi.org/10.4121/eb78267a-137b-4f61-bb7e-6549915a24c7, hosted at the 4TU.ResearchData repository (Chowdhury et al., 2025).

Acknowledgments
This study is part of the Rivers2Morrow research program, which is funded by the Dutch Ministry of Infrastructure and Water Management. We thank Merel C. Verbeek, Max H.I. Schropp, Kees Sloff, Matthew J. Czapiga, and Wiebe de Jong for insightful discussions, and Rijkswaterstaat for sharing measured data. We thank the Editor, Associate Editor, reviewers Lorenzo Durante and Niccolò Ragno, and one anonymous reviewer for their thoughtful feedback.

References

Arkesteijn, L., Blom, A., Czapiga, M. J., Chavarrías, V., & Labeur, R. J. (2019). The quasi-equilibrium longitudinal profile in backwater reaches of the engineered alluvial river: A space-marching method. *Journal of Geophysical Research: Earth Surface*, *124*(11), 2542–2560. https://doi.org/10.1029/2019jf005195

Barile, G., Passalacqua, P., Kwon, S., & Tubino, M. (2025). Controlling factors on water and sediment partitioning at deltaic bifurcations. *Journal of Geophysical Research: Earth Surface*, *130*(7), e2024JF008152. https://doi.org/10.1029/2024JF008152

Barile, G., Redolfi, M., & Tubino, M. (2025). Time scales of river bifurcations. *Earth Surface Processes and Landforms*, *50*(12), e70159. https://doi.org/10.1002/esp.70159

Becker, A. (2021). *Slim suppleren Boven-Waal*. (Tech. Rep. No. 11206792-014-ZWS-0001). Deltares. (in Dutch).

Best, J. (2019). Anthropogenic stresses on the world's big rivers. *Nature Geoscience*, *12*(1), 7–21. https://doi.org/10.1038/s41561-018-0262-x

Blom, A., Arkesteijn, L., Chavarrías, V., & Viparelli, E. (2017). The equilibrium alluvial river under variable flow and its channel-forming discharge. *Journal of Geophysical Research: Earth Surface*, *122*(10), 1924–1948. https://doi.org/10.1002/2017jf004213

Blom, A., Viparelli, E., & Chavarrías, V. (2016). The graded alluvial river: Profile concavity and downstream fining. *Geophysical Research Letters*, *43*(12), 6285–6293. https://doi.org/10.1002/2016gl068898

Blom, A., Ylla Arbós, C., Chowdhury, M. K., Doelman, A., Rietkerk, M., & Schielen, R. M. J. (2024). Indications of ongoing noise-tipping of a bifurcating river system. *Geophysical Research Letters*, *51*(22), e2024GL111846. https://doi.org/10.1029/2024GL111846

Blum, M. D., & Törnqvist, T. E. (2000). Fluvial responses to climate and sea-level change: A review and look forward. *Sedimentology*, *47*(1), 2–48. https://doi.org/10.1046/j.1365-3091.2000.00008.x

Bolla Pittaluga, M., Repetto, R., & Tubino, M. (2003). Channel bifurcation in braided rivers: Equilibrium configurations and stability. *Water Resources Research*, *39*(3). https://doi.org/10.1029/2001wr001112

Buitink, J., Tsiokanos, A., Geertsema, T., Ten Velden, C., Bouaziz, L., & Sperna Weiland, F. (2023). *Implications of the KNMI'23 climate scenarios for the discharge of the Rhine and Meuse*. (Tech. Rep. No. 11209265-002-ZWS-0003). Deltares.

Chadwick, A. J., Lamb, M. P., & Ganti, V. (2020). Accelerated river avulsion frequency on lowland deltas due to sea-level rise. *Proceedings of the National Academy of Sciences*, *117*(30), 17584–17590. https://doi.org/10.1073/pnas.1912351117

Chowdhury, M. K., Blom, A., Ylla Arbós, C., & Schielen, R. M. J. (2025). Schematized model of the lower Rhine River in SOBEK-RE [Dataset]. https://doi.org/10.4121/eb78267a-137b-4f61-bb7e-6549915a24c7

Chowdhury, M. K., Blom, A., Ylla Arbós, C., Verbeek, M. C., Schropp, M. H. I., & Schielen, R. M. J. (2023). Semicentennial response of a bifurcation region in an engineered river to peak flows and human interventions. *Water Resources Research*, *59*(4), e2022WR032741. https://doi.org/10.1029/2022WR032741

Chowdhury, M. K., Konsoer, K. M., & Hiatt, M. (2022). Effect of lateral outflow on three-dimensional flow structure in a river delta. *Water Resources Research*, *58*(10), e2021WR031346. https://doi.org/10.1029/2021wr031346

Cleveland, W. S., & Devlin, S. J. (1988). Locally weighted regression: An approach to regression analysis by local fitting. *Journal of the American Statistical Association*, *83*(403), 596–610. https://doi.org/10.1080/01621459.1988.10478639

Czapiga, M. J., Blom, A., & Viparelli, E. (2022). Efficacy of longitudinal training walls to mitigate riverbed erosion. *Water Resources Research*, *58*(12), e2022WR033072. https://doi.org/10.1029/2022WR033072

Czapiga, M. J., Blom, A., & Viparelli, E. (2022). Sediment nourishments to mitigate channel bed incision in engineered rivers. *Journal of Hydraulic Engineering*, *148*(6), 04022009. https://doi.org/10.1061/(asce)hy.1943-7900.0001977

De Vriend, H. J. (2015). The long-term response of rivers to engineering works and climate change. *Proceedings—Institution of Civil Engineers*, *168*(3), 139–144. https://doi.org/10.1680/cien.14.00068

Dong, T. Y., Nittrouer, J. A., McElroy, B., Il'icheva, E., Pavlov, M., Ma, H., et al. (2020). Predicting water and sediment partitioning in a delta channel network under varying discharge conditions. *Water Resources Research*, *56*(11), e2020WR027199. https://doi.org/10.1029/2020WR027199

Durante, L., Tambroni, N., & Bolla Pittaluga, M. (2025). Multiple equilibrium configurations in river-dominated deltas. *Earth Surface Dynamics*, *13*(3), 455–471. https://doi.org/10.5194/esurf-13-455-2025

Edmonds, D. (2012). Stability of backwater-influenced river bifurcations: A study of the Mississippi-Atchafalaya system. *Geophysical Research Letters*, *39*(8). https://doi.org/10.1029/2012GL051125

Edmonds, D., Caldwell, R. L., Brondizio, E. S., & Siani, S. M. O. (2020). Coastal flooding will disproportionately impact people on river deltas. *Nature Communications*, *11*(1), 4741. https://doi.org/10.1038/s41467-020-18531-4

Edmonds, D., Chadwick, A. J., Lamb, M. P., Lorenzo-Trueba, J., Murray, A. B., Nardin, W., et al. (2022). Morphodynamic modeling of river-dominated deltas: A review and future perspectives. In *Treatise on geomorphology* (pp. 110–140). Elsevier. https://doi.org/10.1016/b978-0-12-818234-5.00076-6

Edmonds, D., Slingerland, R., Best, J., Parsons, D., & Smith, N. (2010). Response of river-dominated delta channel networks to permanent changes in river discharge. *Geophysical Research Letters*, *37*(12). https://doi.org/10.1029/2010GL043269

Frings, R. M. (2011). Sedimentary characteristics of the gravel-sand transition in the River Rhine. *Journal of Sedimentary Research*, *81*(1), 52–63. https://doi.org/10.2110/jsr.2011.2

Frings, R. M., Döring, R., Beckhausen, C., Schüttrumpf, H., & Vollmer, S. (2014). Fluvial sediment budget of a modern, restrained river: The lower reach of the Rhine in Germany. *Catena*, *122*, 91–102. https://doi.org/10.1016/j.catena.2014.06.007

Frings, R. M., & Kleinhans, M. G. (2008). Complex variations in sediment transport at three large river bifurcations during discharge waves in the River Rhine. *Sedimentology*, *55*(5), 1145–1171. https://doi.org/10.1111/j.1365-3091.2007.00940.x

Gruijters, S. H. L. L., Gunnink, J., Hettelaar, J. J. M., De Kleine, M. P. E., Maljers, D., & Veldkamp, J. G. (2003). *Kartering ondergrond IJsselkop, fase 3, eindrapport*. Technical Report No. NITG 03-120-B). Nederlands Instituut voor Toegepaste Geowetenschappen TNO. (in Dutch).

Gruijters, S. H. L. L., Veldkamp, J. G., Gunnink, J., & Bosch, J. H. A. (2001). *De lithologische en sedimentologische opbouw van de ondergrond van de Pannerdensche Kop: Interpretatie van de meetresultaten*. (Technical Report No. NITG 01-166-B). Nederlands Instituut voor Toegepaste Geowetenschappen TNO. (in Dutch).

Hackney, C. R., Darby, S. E., Parsons, D. R., Leyland, J., Aalto, R., Nicholas, A. P., & Best, J. L. (2017). The influence of flow discharge variations on the morphodynamics of a diffluence-confluence unit on a large river. *Earth Surface Processes and Landforms*, *43*(2), 349–362. https://doi.org/10.1002/esp.4204

Hirano, M. (1971). River-bed degradation with armoring. *Proc. Japan Society of Civil Engineers*, *195*, 55–65. https://doi.org/10.2208/jscej1969.1971.195_55

Hoyal, D. C. J. D., & Sheets, B. A. (2009). Morphodynamic evolution of experimental cohesive deltas. *Journal of Geophysical Research*, *114*(F2). https://doi.org/10.1029/2007jf000882

IPCC. (2023). Weather and climate extreme events in a changing climate. In *Climate change 2021 – The physical science basis* (pp. 1513–1766). Cambridge University Press. (Contribution of Working Group I to the Sixth Assessment Report of the Intergovernmental Panel on Climate Change). https://doi.org/10.1017/9781009157896.006

Kleinhans, M. G., Ferguson, R. I., Lane, S. N., & Hardy, R. J. (2013). Splitting rivers at their seams: Bifurcations and avulsion. *Earth Surface Processes and Landforms*, *38*(1), 47–61. https://doi.org/10.1002/esp.3268

Kleinhans, M. G., Jagers, H. R. A., Mosselman, E., & Sloff, C. J. (2008). Bifurcation dynamics and avulsion duration in meandering rivers by one-dimensional and three-dimensional models. *Water Resources Research*, *44*(8). https://doi.org/10.1029/2007wr005912

Liang, M., Van Dyk, C., & Passalacqua, P. (2016). Quantifying the patterns and dynamics of river deltas under conditions of steady forcing and relative sea level rise. *Journal of Geophysical Research: Earth Surface*, *121*(2), 465–496. https://doi.org/10.1002/2015JF003653

Masson-Delmotte, V., Zhai, P., Pirani, A., Connors, S. L., Péan, C., Chen, Y., et al. (Eds.). (2023). *Climate change 2021 – The physical science basis: Working Group I contribution to the sixth assessment report of the intergovernmental panel on climate change*. Cambridge University Press. https://doi.org/10.1017/9781009157896

Miori, S., Repetto, R., & Tubino, M. (2006). A one-dimensional model of bifurcations in gravel bed channels with erodible banks. *Water Resources Research*, *42*(11). https://doi.org/10.1029/2006wr004863

Mulatu, C. A., Crosato, A., Langendoen, E. J., Moges, M. M., & McClain, M. E. (2020). Long-term effects of dam operations for water supply to irrigation on downstream river reaches. The case of the Ribb River, Ethiopia. *International Journal of River Basin Management*, *19*(4), 429–443. https://doi.org/10.1080/15715124.2020.1750421

O'Neill, B. C., Kriegler, E., Ebi, K. L., Kemp-Benedict, E., Riahi, K., Rothman, D. S., et al. (2017). The roads ahead: Narratives for shared socioeconomic pathways describing world futures in the 21st century. *Global Environmental Change*, *42*, 169–180. https://doi.org/10.1016/j.gloenvcha.2015.01.004

Ottevanger, W., Giri, S., & Sloff, C. J. (2015). *Sustainable fairway rhinedelta II*. (Tech. Rep. No. 1209175-000-ZWS-0020). Deltares.

Parker, G., & Andrews, E. D. (1985). Sorting of bed load sediment by flow in meander bends. *Water Resources Research*, *21*(9), 1361–1373. https://doi.org/10.1029/wr021i009p01361

Parker, G., & Sutherland, A. J. (1990). Fluvial armor. *Journal of Hydraulic Research*, *28*(5), 529–544. https://doi.org/10.1080/00221689009499044

Quick, I., König, F., Baulig, Y., Schriever, S., & Vollmer, S. (2020). Evaluation of depth erosion as a major issue along regulated rivers using the classification tool Valmorph for the case study of the Lower Rhine. *International Journal of River Basin Management*, *18*(2), 191–206. https://doi.org/10.1080/15715124.2019.1672699

Ragno, N., Redolfi, M., Tambroni, N., & Tubino, M. (2023). Modeling steady grain sorting in river bifurcations. *Journal of Geophysical Research: Earth Surface*, *128*(9), e2023JF007230. https://doi.org/10.1029/2023jf007230

Ragno, N., Tambroni, N., & Bolla Pittaluga, M. (2022). Competing feedback in an idealized tide-influenced delta network. *Environmental Fluid Mechanics*, *22*(2–3), 535–557. https://doi.org/10.1007/s10652-022-09857-2

Saint Venant, A. J. C. B. (1871). Théorie du mouvement non permanent des eaux, avec application aux crues des rivières et à l'introduction de marées dans leur lit. *Comptes Rendus de l'Académie des Sciences de Paris*, *73*(99), 237–240. (in French).

Salter, G., Paola, C., & Voller, V. R. (2018). Control of delta avulsion by downstream sediment sinks. *Journal of Geophysical Research: Earth Surface*, *123*(1), 142–166. https://doi.org/10.1002/2017jf004350

Salter, G., Voller, V. R., & Paola, C. (2020). Chaos in a simple model of a delta network. *Proceedings of the National Academy of Sciences*, *117*(44), 27179–27187. https://doi.org/10.1073/pnas.2010416117

Schielen, R. M. J., & Blom, A. (2018). A reduced complexity model of a gravel-sand river bifurcation: Equilibrium states and their stability. *Advances in Water Resources*, *121*, 9–21. https://doi.org/10.1016/j.advwatres.2018.07.010

Schumm, S. A. (1993). River response to baselevel change: Implications for sequence stratigraphy. *The Journal of Geology*, *101*(2), 279–294. https://doi.org/10.1086/648221

Sloff, C. J. (2006). *Uitbreiding SOBEK-RE model NAAR NIET-uniform sediment*. (Tech. Rep. No. Q4130). Delft Hydraulics. (in Dutch).

Sloff, C. J., & Mosselman, E. (2012). Bifurcation modelling in a meandering gravel-sand bed river. *Earth Surface Processes and Landforms*, *37*(14), 1556–1566. https://doi.org/10.1002/esp.3305

Stahl, K., Weiler, M., Van Tiel, M., Kohn, I., Hänsler, A., Freudiger, D., et al. (2022). *Impact of climate change on the rain, snow and glacier melt components of streamflow of the river Rhine and its tributaries*. Tech. Rep. (Vol. 28). International Commission for the Hydrology of the Rhine Basin (CHR).

Szupiany, R. N., Amsler, M. L., Hernandez, J., Parsons, D. R., Best, J. L., Fornari, E., & Trento, A. (2012). Flow fields, bed shear stresses, and suspended bed sediment dynamics in bifurcations of a large river. *Water Resources Research*, *48*(11). https://doi.org/10.1029/2011wr011677

Ten Brinke, W. B. M. (2005). *The Dutch Rhine: A restrained river*. Veen Magazines.

Tessler, Z. D., Vörösmarty, C. J., Overeem, I., & Syvitski, J. P. M. (2018). A model of water and sediment balance as determinants of relative sea level rise in contemporary and future deltas. *Geomorphology*, *305*, 209–220. https://doi.org/10.1016/j.geomorph.2017.09.040

Van de Lageweg, W., & Slangen, A. (2017). Predicting dynamic coastal delta change in response to sea-level rise. *Journal of Marine Science and Engineering*, *5*(2), 24. https://doi.org/10.3390/jmse5020024

Van der Mark, C. F., & Mosselman, E. (2013). Effects of helical flow in one-dimensional modelling of sediment distribution at river bifurcations. *Earth Surface Processes and Landforms*, *38*(5), 502–511. https://doi.org/10.1002/esp.3335

Van der Zwaard, J. J. (1981). *Splitsingspunt Pannerdense Kop; Verdeling van het sedimenttransport bij het splitsingspunt*. (Tech. Rep. No. M932). Waterloopkundig Laboratorium. (in Dutch).

Van de Wiel, M. J., Coulthard, T. J., Macklin, M. G., & Lewin, J. (2011). Modelling the response of river systems to environmental change: Progress, problems and prospects for Palaeo-environmental reconstructions. *Earth-Science Reviews*, *104*(1–3), 167–185. https://doi.org/10.1016/j.earscirev.2010.10.004

Van Dorland, R., Beersma, J., Bessembinder, J., Bloemendaal, N., Van den Brink, H., Brotons Blanes, H., et al. (2023). KNMI national climate scenarios 2023 for the Netherlands (Tech. Rep. No. WR23-02).

Van Verseveld, W. J., Weerts, A. H., Visser, M., Buitink, J., Imhoff, R. O., Boisgontier, H., et al. (2024). Wflow-SBM v0.7.3, a spatially distributed hydrological model: From global data to local applications. *Geoscientific Model Development*, *17*(8), 3199–3234. https://doi.org/10.5194/gmd-17-3199-2024

Viparelli, E., Haydel, R., Salvaro, M., Wilcock, P. R., & Parker, G. (2010). River morphodynamics with creation/consumption of grain size stratigraphy, 1: Laboratory experiments. *Journal of Hydraulic Research*, *48*(6), 715–726. https://doi.org/10.1080/00221686.2010.515383

Viparelli, E., Sequeiros, O. E., Cantelli, A., Wilcock, P. R., & Parker, G. (2010). River morphodynamics with creation/consumption of grain size stratigraphy, 2: Numerical model. *Journal of Hydraulic Research*, *48*(6), 727–741. https://doi.org/10.1080/00221686.2010.526759

Wang, Z. B., De Vries, M., Fokkink, R. J., & Langerak, A. (1995). Stability of river bifurcations in 1D morphodynamic models. *Journal of Hydraulic Research*, *33*(6), 739–750. https://doi.org/10.1080/00221689509498549

Woodruff, J. D., Irish, J. L., & Camargo, S. J. (2013). Coastal flooding by tropical cyclones and sea-level rise. *Nature*, *504*(7478), 44–52. https://doi.org/10.1038/nature12855

Ylla Arbós, C., Blom, A., Sloff, C. J., & Schielen, R. M. J. (2023). Centennial channel response to climate change in an engineered river. *Geophysical Research Letters*, *50*(8), e2023GL103000. https://doi.org/10.1029/2023GL103000

Ylla Arbós, C., Blom, A., Viparelli, E., Reneerkens, M., Frings, R. M., & Schielen, R. M. J. (2021). River response to anthropogenic modification: Channel steepening and gravel front fading in an incising river. *Geophysical Research Letters*, *48*(4), e2020GL091338. https://doi.org/10.1029/2020GL091338

Zolezzi, G., Bertoldi, W., & Tubino, M. (2006). Morphological analysis and prediction of river bifurcations. Braided Rivers: Process, deposits. *Ecological Management*, *36*, 233–256. https://doi.org/10.1002/9781444304374.ch11

References From the Supporting Information

Arkesteijn, L., Blom, A., & Labeur, R. J. (2021). A rapid method for modeling transient river response under stochastic controls with applications to sea level rise and sediment nourishment. *Journal of Geophysical Research: Earth Surface*, *126*(12), e2021JF006177. https://doi.org/10.1029/2021jf006177

Arnold, G., Bos, H., Doef, R., Kielen, N., & Luijn, F. v. (2009). *Waterhuishouding en waterverdeling in Nederland (No. 382306)*. Ministerie van Verkeer en Waterstaat, Rijkswaterstaat. (in Dutch).

Ashida, K., & Michiue, M. (1972). Study on hydraulic resistance and bed-load transport rate in alluvial streams. In *Proceedings of the Japan Society for Comparative Endocrinology*. (Vol. 206, pp. 59–69). Proceedings of the Japan Society of Civil Engineers. (in Japanese). https://doi.org/10.2208/jscej1969.1972.206_59

Bamber, J. L., Oppenheimer, M., Kopp, R. E., Aspinall, W. P., & Cooke, R. M. (2019). Ice sheet contributions to future sea-level rise from structured expert judgment. *Proceedings of the National Academy of Sciences*, *116*(23), 11195–11200. https://doi.org/10.1073/pnas.1817205116

Becker, A. (2020). *Tweede suppletie Boven-Rijn: Tussenevaluatie hoogwater 2020*. (Tech. Rep. No. 11205234-010-ZWS-0001). Deltares. (in Dutch).

Bresse, J. A. C. (1860). *Cours de mécanique appliquée* (Vol. 2). Mallet-Bachelier. (in French).

De Vries, M. (1994). Unsolved problems in one-dimensional morphological models. In *IAHR-AD*. IAHR.

DeConto, R. M., Pollard, D., Alley, R. B., Velicogna, I., Gasson, E., Gomez, N., et al. (2021). The Paris climate agreement and future sea-level rise from Antarctica. *Nature*, *593*(7857), 83–89. https://doi.org/10.1038/s41586-021-03427-0

Deltares. (2012). *Flow—Technical reference manual SOBEK RE 2.52.008*. (Tech. Rep.). Delft.

Egiazaroff, I. V. (1965). Calculation of nonuniform sediment concentrations. *Journal of the Hydraulics Division*, *91*(4), 225–247. https://doi.org/10.1061/JYCEAJ.0001277

Frings, R. M., Hillebrand, G., Gehres, N., Banhold, K., Schriever, S., & Hoffmann, T. (2019). From source to mouth: Basin-scale morphodynamics of the Rhine River. *Earth-Science Reviews*, *196*, 102830. https://doi.org/10.1016/j.earscirev.2019.04.002

International Commission for the Protection of the Rhine. (2020). *ICPR Rhine atlas 2020*. Retrieved from https://geoportal.bafg.de/karten/rhineatlas/

Lokin, L. R., Warmink, J. J., Bomers, A., & Hulscher, S. J. M. H. (2022). River dune dynamics during low flows. *Geophysical Research Letters*, *49*(8), e2021GL097127. https://doi.org/10.1029/2021GL097127

Meyer-Peter, E., & Müller, R. (1948). Formulas for bed load transport. In *Proceedings. 2nd Meeting international association for hydraulic structures research* (pp. 39–64). Delft.

Niesten, I., Ottevanger, W., & Becker, A. (2017). *Riviersuppleties in de Rijntakken- Conclusies 1e suppletie Boven-Rijn en advies voortzetting monitoring*. (Tech. Rep. No. 11200877-000-ZWS-0005). Deltares. (in Dutch).

Parker, G. (2008). Transport of gravel and sediment mixtures. In *Sedimentation engineering* (pp. 165–251). American Society of Civil Engineers. https://doi.org/10.1061/9780784408148.ch03

Rijkswaterstaat. (1968). *De waterhuishouding van Nederland 1968 (Eerste Nota Waterhuishouding) (No. 196530)*. Ministerie van Verkeer en Waterstaat, Rijkswaterstaat. (in Dutch).

Rijkswaterstaat. (1985). *De waterhuishouding van Nederland 1984 (Tweede Nota Waterhuishouding) (No. 229140)*. Ministerie van Verkeer en Waterstaat, Rijkswaterstaat. (in Dutch).

Rijkswaterstaat. (1987). *Een peilregeling voor de combinatie stuw Amerongen—waterkrachtcentrale Maurik (No. 112300)*. Ministerie van Verkeer en Waterstaat, Rijkswaterstaat, Directie Gelderland (RWS, GL). (Nota AXP 87.01, in Dutch).

Rijkswaterstaat. (1991). *Derde nota waterhuishouding: Voortgangsrapportage 1991 (No. 180862)*. Ministerie van Verkeer en Waterstaat, Rijkswaterstaat. (in Dutch).

Rijkswaterstaat. (1998). *Vierde Nota waterhuishouding: Regeringsbeslissing (No. 228836)*. Ministerie van Verkeer en Waterstaat, Rijkswaterstaat. (in Dutch).

Rijkswaterstaat. (2009). *Beheer-en ontwikkelplan voor de Rijkswateren 2010–2015: Werken aan een robuust watersysteem (No. 396037)*. Ministerie van Verkeer en Waterstaat, Rijkswaterstaat. (in Dutch).

Rijkswaterstaat. (2015). *Beheer-en ontwikkelplan Voor de Rijkswateren 2016–2021 (No. 824359)*. Ministerie van Verkeer en Waterstaat, Rijkswaterstaat. (in Dutch).

Rijkswaterstaat. (2018). *Peilbesluit IJsselmeergebied*. (Tech. Rep. No. 814299). Ministerie van Infrastructuur en Waterstaat (Rijkswaterstaat). (in Dutch).

Van der Mark, C. F., Blom, A., & Hulscher, S. M. J. H. (2008). Quantification of variability in bedform geometry. *Journal of Geophysical Research*, *113*(3). https://doi.org/10.1029/2007JF000940

Van Doornik, W., Den Daas, J., Pfaff-Wagenaar, M., Dorenbosch, M., Liefveld, W., & Grutters, B. (2019). *Stuwbeheer Nederrijn–Lek: optimalisatiestudie vanuit de KRW-functie*. (Tech. Rep.). Rijkswaterstaat. (in Dutch).

Ylla Arbós, C., Blom, A., White, S. R., Patzwahl, R., & Schielen, R. M. J. (2024). Large-scale channel response to erosion-control measures. *Water Resources Research*, *60*(3), e2023WR036603. https://doi.org/10.1029/2023wr036603